
Estimating Long-term Heterogeneous Dose-response Curve: Generalization Bound Leveraging Optimal Transport Weights

Ze Qin Yang^{1*} Weilin Chen^{1*} Ruichu Cai^{1,2†} Yuguang Yan¹ Zhifeng Hao³

Zhipeng Yu⁴ Zhichao Zou⁴ Peng Zhen⁴ Jiecheng Guo⁴

¹ School of Computer Science, Guangdong University of Technology

² Pazhou Laboratory (Huangpu)

³ College of Science, Shantou University

⁴ Didi Chuxing

{youngzeqin, chenweilin.chn, cairuichu}@gmail.com

ygyan@gdut.edu.cn, haozhifeng@stu.edu.cn

{yuzhipeng, zouzhichao, zhenpeng, jasonguo}@didiglobal.com

Abstract

Long-term causal effect estimation is a significant but challenging problem in many applications. Existing methods rely on ideal assumptions to estimate long-term average effects, e.g., no unobserved confounders or a binary treatment, while in numerous real-world applications, these assumptions could be violated and average effects are unable to provide individual-level suggestions. In this paper, we address a more general problem of estimating the long-term heterogeneous dose-response curve (HDRC) while accounting for unobserved confounders. Specifically, to remove unobserved confounding in observational data, we introduce an optimal transport weighting framework to align the observational data to the experimental data with theoretical guarantees. Furthermore, to accurately predict the heterogeneous effects of continuous treatment, we establish a generalization bound on counterfactual prediction error by leveraging the reweighted distribution induced by optimal transport. Finally, we develop an HDRC estimator building upon the above theoretical foundations. Extensive experimental studies conducted on multiple synthetic and semi-synthetic datasets demonstrate the effectiveness of our proposed method.

1 Introduction

Long-term causal inference is practically significant across many domains [27, 19, 13]. Randomized control experiments are the gold standard for estimating causal effects. However, it is practically difficult or even impossible to collect the long-term outcome of interest through experiments due to cost considerations, e.g., taking years or even decades of follow-up to fully reveal mortality in acquired immunodeficiency syndrome drug clinical trials. In contrast, long-term observational data are often easier or cheaper to acquire, and thus the long-term observational data has been taken as the complementary of short-term experimental data. A typical causal graph of long-term effect estimation is shown in Fig. 1a, where short-term experimental and long-term observational data are accessible.

There has been considerable interest in using short-term outcomes as replacement or supplement for the long-term outcome in different ways via data combination. With all observed confounders,

*Equal contributions

†Corresponding authors.

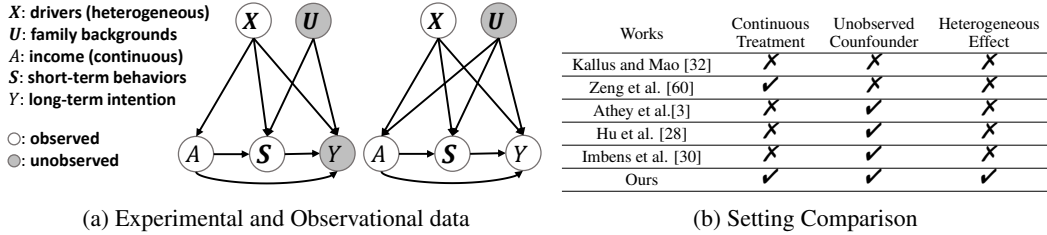


Figure 1: Fig. 1a are typical causal graphs of experimental and observational data in long-term effect estimation scenarios. Fig. 1a shows a ride-hailing scenario where treatment A is continuous and unobserved confounders U exist. Table 1b shows the differences between existing works and ours.

[32] focuses on a binary treatment setting, showing the benefit of short-term outcomes in estimating average long-term effects. Further, [60] extends it to the continuous treatment setting. As a counterpart, allowing the existence of unobserved confounders, [3, 28, 30] assume that short-term outcomes, to some extent, capture the information of unobserved confounders to deal with the confounding problem, nevertheless, they still all focus on estimating average effect of binary treatment.

Previous works, however, lack practical applicability, since they have largely focused on estimating average treatment effects under ideal assumptions, e.g., no unobserved confounders in observational data or binary treatment, as shown in Table 1b. In many long-run applications, such assumptions may be violated. Decision-makers usually leverage long-term individual-level effects estimated with unobserved confounders and continuous treatment to develop policies for individuals. For the example shown in Fig. 1a, in a ride-hailing platform, in order to increase drivers' long-term retention (*long-term outcome*), the platform has to evaluate the effect of various incomes (*continuous treatment*) of different drivers (*heterogeneity*). For effect estimation, the platform can conduct short-term experiments to obtain drivers' short-term behaviors (*short-term outcomes*) and collect historical long-term observational data. In the observational data, even though short/long-term outcomes can all be observed, confounders are partially observed due to information privacy, e.g., drivers' family backgrounds (*unobserved confounders*). In such an application, with unobserved confounders, it is still understudied how to accurately estimate the long-term effect of various incomes on the long-term retention of specific drivers, i.e., heterogeneous dose-response curve (HDRC), via data combination.

Motivated by the example above, in this paper, we focus on estimating long-term HDRC with unobserved confounders via data combination as shown in Table 1b. Long-term heterogeneous effect estimation poses significant challenges, primarily due to the unobserved confounders in the observational dataset and the lack of counterfactual outcomes in estimating the heterogeneous curves of continuous treatment. Specifically, the first and biggest challenge is that the long-term outcome only exists in the observational dataset with unobserved confounders and is missing in the experimental dataset, causing the identification problem. The second challenge is that since treatment is continuous, the short and long-term counterfactual outcomes are potentially infinite, causing a large counterfactual prediction error in estimating the heterogeneous curves with only the actual outcome. Our solution and contribution can be summarized as follows:

- We address the problem of estimating long-term heterogeneous dose-response curves with unobserved confounders via data combination. To the best of our knowledge, this is the first work to address this problem as shown in Table 1b.
- We theoretically show that the unobserved confounding can be removed by aligning the conditional distributions of short-term outcomes between observational and experimental groups. To achieve such alignment, under a reweighting framework of optimal transport (OT), we establish a mini-batch and joint distribution-based upper bounds on the discrepancy of conditional distributions
- Based on the OT-induced weighted distribution, we derive the generalization bound on the counterfactual prediction error in estimating long-term HDRC, which inspires our final model, called Long-term heterogeneous dose-response curve estimator with Reweighting and representation learning (LEARN).

2 Related Work

Optimal Transport Recently, optimal transport has shown powerful abilities in different kinds of applications, such as computer vision [26, 21, 38, 48], domain adaption [14, 15, 17, 10], generative models [29, 22, 37, 1] and so on. There are also some works trying to introduce optimal transport into causal inference. [25] employs unbalanced optimal transport for matching. [39] proposes to infer counterfactual outcomes via transporting the factual distribution to the counterfactual one. [18, 58] apply optimal transport to learn sample weights to achieve distribution balancing. [55] solves the problems of mini-batch sampling and unobserved confounders in CFR [46] through optimal transport. To the best of our knowledge, this is the first work exploiting optimal transport to solve the unobserved confounder problem via data combination under the long-term estimation scenario.

Long-term Causal Inference To date, a common approach to estimating long-term causal effects is based on short-term outcomes. By making an additional surrogacy assumption that short-term outcomes can mediate the full effect of treatment, [2] combines multiple short-term outcomes to robustly estimate the average long-term effects, [12] adapt RNN to learn the relationship between the short-term and long-term outcomes. However, the surrogacy assumption can be easily violated in practice. In this setting, [32] investigates the role of short-term outcomes for long-term causal inference and [60] serves as a counterpart for [32] in the continuous treatment setting. [9] considers a more realistic scenario where some valid surrogates are unobserved and employ an identifiable variational autoencoder to recover them. Further, To solve the unobserved confounder problem, [3] proposes a relaxed latent unconfoundedness assumption, and proposes different estimators based on the imputation, weighting, and control function methods. [23] proposes other feasible assumptions to replace the assumption used in [3]. [30] exploits the sequential structure of short-term outcomes and develops a proximal learning-based method. [50] performs instrumental variable regression to estimate average long-term effects. Although many different settings of long-term effect estimation have been explored, to the best of our knowledge, we are the first to focus on the long-term HDRC estimation problem with unobserved confounders.

3 Preliminary

3.1 Optimal Transport Weighting

Optimal transport (OT) [52] is widely used to quantify distribution discrepancy as the minimum cost of transporting one distribution to another. Among the rich theory of OT, we focus on the *Kantorovich Problem* [33] for discrete distribution in this paper. Recently, thanks to its many advantages, such as geometric sensitivity and stability, OT has been explored for learning weights to align distribution [18, 58, 26] and demonstrated excellent performance. Specifically, suppose we want to learn weights \mathbf{w}_α for samples in distribution α , such that the reweighted distribution is aligned with another distribution β . To achieve this goal, we view the to-be-learned weights \mathbf{w}_α as the probability measure of distribution α , and represent the distribution β with a uniform probability measure $\boldsymbol{\mu}$. By doing so, the learning of \mathbf{w}_α can be formulated as the process of minimizing the OT distance between distributions α and β :

$$\begin{aligned} \min_{\mathbf{w}_\alpha} OT(\alpha, \beta) &= \min_{\mathbf{w}_\alpha} \min_{\Gamma \in \Pi(\alpha, \beta)} \langle \Gamma, C \rangle, \\ s.t. \quad \Pi(\alpha, \beta) &= \{ \Gamma \in \mathbb{R}^{n \times m} \mid \Gamma \mathbf{1}_m = \mathbf{w}_\alpha, \Gamma^T \mathbf{1}_n = \boldsymbol{\mu}, \Gamma_{ij} \in [0, 1] \} \end{aligned} \quad (1)$$

where $\langle \cdot, \cdot \rangle$ is the Frobenius inner product, n and m are the sample numbers of distribution α and β , the transport cost matrix C is the unit-wise distance between α and β , the transport probability matrix Γ satisfying $\Pi(\alpha, \beta)$ is learned by minimizing $OT(\alpha, \beta)$, which reflects how to transport samples from the distribution α to β .

3.2 Long-term Heterogeneous Dose-response Curve

Let $A \in \mathcal{A}$ be the 1-dimensional continuous treatment, $\mathbf{X} \in \mathcal{X}$ be the observed covariates, $\mathbf{U} \in \mathcal{U}$ be the unobserved covariates, $\mathbf{S}(a) \in \mathcal{S}$ be the potential short-term outcomes measured at timesteps $1, 2, \dots, t_0$, and $Y(a) \in \mathcal{Y}$ be the potential long-term outcome measured at timestep T . Let lowercase letters (e.g., $a, \mathbf{x}, \mathbf{u}, \mathbf{s}(a), y(a)$) denote the value of the above random variables. Following potential

outcome framework [44], the observed short and long-term outcomes \mathbf{S}, Y are the potential outcomes $\mathbf{S}(a), Y(a)$ corresponding to the actually received treatment a .

Following [3, 11, 23, 30], we consider a data combination setting where $G = \{o, e\}$ distinguishes between two types of datasets: a large observational dataset $O = \{a_i, \mathbf{x}_i, \mathbf{s}_i, y_i, G_i = o\}_{i=1}^{n_o}$ and a small experimental dataset $E = \{a_i, \mathbf{x}_i, \mathbf{s}_i, G_i = e\}_{i=1}^{n_e}$ ($n_e \ll n_o$). That is, the treatment A , covariates \mathbf{X} and short-term outcomes \mathbf{S} are available in both datasets, while long-term outcome Y is only available in observational dataset. Our goal is to estimate the long-term heterogeneous dose-response curve (HDRC), which is defined as:

$$\mu(\mathbf{x}, a) = \mathbb{E}[Y(a)|\mathbf{X} = \mathbf{x}]. \quad (2)$$

Notably, the long-term HDRC cannot be estimated solely from the experimental dataset due to the missingness of long-term outcome Y , and also cannot be estimated solely from the observational dataset due to the possible unobserved confounders \mathbf{U} . To overcome these challenges, we learn long-term HDRC via data combination, requiring the following assumptions:

Assumption 1 (Consistency, Positivity). *If $A = a$, we have $Y = Y(a)$, $\mathbf{S} = \mathbf{S}(a)$. And $\forall a, x$, we have $0 < P(A = a|\mathbf{X} = \mathbf{x}) < 1$, $0 < P(G = o|A = a, \mathbf{X} = \mathbf{x}) < 1$.*

Assumption 2 (Weak internal validity of observational data). $A \perp\!\!\!\perp \{Y(a), \mathbf{S}(a)|\mathbf{X}, \mathbf{U}, G = o$.

Assumption 3 (Internal validity of experimental data). $A \perp\!\!\!\perp \{Y(a), \mathbf{S}(a)|\mathbf{X}, G = e$.

Assumption 4 (External validity of experimental data). $G \perp\!\!\!\perp \{Y(a), \mathbf{S}(a)|\mathbf{X}$.

Assumption 5 (Latent Unconfoundedness). $A \perp\!\!\!\perp Y(a)|\mathbf{X}, \mathbf{S}(a), G = o$.

The assumptions above are mild and widely used in existing literature, e.g., [3, 23]. Assumption 1 is a standard and basis assumption. Importantly, Assumption 2 allows unobserved confounders to exist in the observational dataset, and Assumption 3 guarantees that the treatment in the experimental dataset is unconfounded after controlling the covariates. Assumption 4 allows us to generalize the conditional distribution of potential outcomes between different groups G . Assumption 5 is proposed by [3] to achieve average long-term effect identification under a binary-treatment setting. Different from them, we reuse this assumption to identify HDRC by a novel reweighting method.

4 Proposed Method

To estimate long-term HDRC, we present our method exploiting reweighting to handle the unobserved confounders and representation learning to handle the observed confounders, respectively. In section 4.1, we first propose a novel weighting technique that can deal with the unobserved confounders in the observational dataset, making HDRC identifiable. We then provide a practical and computationally efficient OT method with theoretical guarantees to learn such weights via data combination. In section 4.2, we derive the generalization bound on counterfactual regression error to address the bias caused by the observed confounders based on the reweighted observational distribution.

4.1 Learning Optimal Transport Weights for Unobserved Confounders via Data Combination

4.1.1 Identifiable Long-term HDRC via Reweighting

We first study how to identify the long-term HDRC. Given that Y is only observed in the observational dataset, identifying HDRC requires the unconfoundedness assumption in the observational dataset, i.e., $A \perp\!\!\!\perp \{\mathbf{S}(a), Y(a)|\mathbf{X}, G = o$, which is unsatisfied as stated in Assumption 2. Fortunately, $A \perp\!\!\!\perp \{\mathbf{S}(a), Y(a)|\mathbf{X}, G = e$ holds, though Y is missing in the experimental dataset. It raises a question: can we remove the unobserved confounding in the observational dataset to achieve identification, by utilizing the experimental dataset which includes only short-term outcomes? We find that, even though \mathbf{U} is unobserved, its influence can be captured by the (in)dependence between \mathbf{S} and G conditional on \mathbf{X} and A , as illustrated in the following proposition.

Proposition 1. *Under Assumptions 1, 2, 3 4, and 5, given a set of weights $\mathbf{w} = \{\mathbf{w}_o, \boldsymbol{\mu}\}$ consisting of the learnable weights \mathbf{w}_o for observational units and uniform weights $\boldsymbol{\mu}$ for experimental units, which makes $\mathbf{w}P(\mathbf{S}, G|\mathbf{X}, A) = P^{\mathbf{w}}(\mathbf{S}, G|\mathbf{X}, A) = P^{\mathbf{w}}(\mathbf{S}|\mathbf{X}, A)P^{\mathbf{w}}(G|\mathbf{X}, A)$, i.e., $\mathbf{S} \perp\!\!\!\perp G|\mathbf{X}, A$, then $\mathbb{E}[\mathbf{S}(a)|\mathbf{X}, A = a, G = o] = \mathbb{E}[\mathbf{S}(a)|\mathbf{X}, G = o]$ holds on the weighted observational distribution.*

The proof is given in Appendix A.1. Proposition 1 is intuitive. Since unconfoundedness holds in $G = e$, then $P(\mathbf{S}(a)|\mathbf{X}, G = e) = P(\mathbf{S}|\mathbf{X}, A = a, G = e)$, but it does not hold when $G = o$. If we can learn weight \mathbf{w} aligning short-term outcomes between observational data and experimental data, i.e., making $P(\mathbf{S}|\mathbf{X}, A, G = e) = P(\mathbf{S}|\mathbf{X}, A, G = o)$, the unconfoundedness condition will also hold in $G = o$ based on Assumption 4. Proposition 1 provides an effective way to remove the unobserved confounding in observational dataset $G = o$. Based on Proposition 1, we can further show HDRC is identifiable as follows.

Theorem 1. *Suppose Assumptions in Proposition 1 hold, we have the unconfoundedness $\mathbb{E}[Y(a)|\mathbf{X}, A = a, G = o] = \mathbb{E}[Y(a)|\mathbf{X}, G = o]$, then the long-term HDRC can be identified.*

The proof is given in Appendix A.2. Theorem 1 is built on Proposition 1, indicating that if we could learn suitable weights making $\mathbf{S} \perp\!\!\!\perp G|\mathbf{X}, A$, the unobserved confounding will be removed, and then long-term HDRC can be identified. Therefore, our goal now is to learn a set of weights \mathbf{w}_o for observational units such that the conditional independence $\mathbf{S} \perp\!\!\!\perp G|\mathbf{X}, A$ holds based on the reweighted distribution, i.e., $P^{\mathbf{w}_o}(\mathbf{S}|\mathbf{X}, A, G = o) = P^\mu(\mathbf{S}|\mathbf{X}, A, G = e)$.

4.1.2 Learning Optimal Transport Weights

Based on the above theoretical analyses, we need learn weights \mathbf{w}_o for observational units to minimize the distances between $P(\mathbf{S}|\mathbf{X}, A, G = o)$ and $P(\mathbf{S}|\mathbf{X}, A, G = e)$. However, most existing works study how to measure the distances between (joint) distributions, instead of conditional distributions. Surprisingly, we find that under the optimal transport framework, the distance between conditional distributions can be bounded by that of joint distributions. As a result, we propose a mini-batch joint distribution-based OT method that not only helps align the above conditional distributions but also can be easily embedded into the training of deep learning with theoretical guarantees.

To begin with, following the objective function in Eq. (1), we model our goal as a problem of minimizing the *conditional OT distance*, i.e., $OT(P(\mathbf{S}|\mathbf{X}, A, G = o), P(\mathbf{S}|\mathbf{X}, A, G = e))$. The intuitive approach to solve this problem is to minimize every sub-problem $OT(P(\mathbf{S}|\mathbf{X} = \mathbf{x}, A = a, G = o), P(\mathbf{S}|\mathbf{X} = \mathbf{x}, A = a, G = e))$ for every realization $\mathbf{X} = \mathbf{x}, A = a$ as follows:

$$OT_{\mathbf{x},a}^{con} = \sum_{\mathbf{x},a} OT(P(\mathbf{S}|\mathbf{X} = \mathbf{x}, A = a, G = o), P(\mathbf{S}|\mathbf{X} = \mathbf{x}, A = a, G = e)). \quad (3)$$

The First Challenge However, solving the above conditional OT problem is infeasible. The reason is that the conditional set (\mathbf{X}, A) in our conditional OT distance are multi-dimensional continuous variables, leading to the existence of infinitely sub-problems in Eq. (3). To overcome this challenge, we establish a connection between the OT distance regarding conditional distributions and that regarding joint distributions:

Theorem 2. *Assuming the cost matrix of the joint distribution $P(\mathbf{S}, \mathbf{X}, A)$ is separable, i.e., $C(\mathbf{s}, \mathbf{x}, a; \tilde{\mathbf{s}}, \tilde{\mathbf{x}}, \tilde{a}) = C(\mathbf{s}; \tilde{\mathbf{s}}) + C(\mathbf{x}; \tilde{\mathbf{x}}) + C(a; \tilde{a})$, we have:*

$$OT_{\mathbf{x},a}^{con} \leq OT(P(\mathbf{S}, \mathbf{X}, A|G = o), P(\mathbf{S}, \mathbf{X}, A|G = e)). \quad (4)$$

In addition, under the positivity assumption, we have $OT(P(\mathbf{S}, \mathbf{X}, A|G = o), P(\mathbf{S}, \mathbf{X}, A|G = e)) \rightarrow 0$ as $n_o \rightarrow \infty$, leading to $OT_{\mathbf{x},a}^{con} \rightarrow 0$.

The proof can be found in Appendix A.3. Theorem 2 shows that the conditional OT distance can be bounded by the OT distance between the corresponding joint distributions, which motivates us to learn weights \mathbf{w}_o by minimizing the upper bound $OT(P(\mathbf{S}, \mathbf{X}, A|G = o), P(\mathbf{S}, \mathbf{X}, A|G = e))$ instead of the infeasible $OT_{\mathbf{x},a}^{con}$. And when $n_o \rightarrow \infty$, the convergence property $OT_{\mathbf{x},a}^{con} \rightarrow 0$ means that the probability measure \mathbf{w}_o of the observational distribution $P^{\mathbf{w}_o}(\mathbf{S}|\mathbf{X}, A, G = o)$ will converge to that of experimental distribution $P(\mathbf{S}|\mathbf{X}, A, G = e)$, ensuring HDRC identifiable based on Proposition 1.

The Second Challenge While we solve the problem of conditional OT, another challenge emerges. Specifically, solving $OT(P(\mathbf{S}, \mathbf{X}, A|G = o), P(\mathbf{S}, \mathbf{X}, A|G = e))$ will cause a high computational cost since the whole optimized transport matrix $\Gamma \in \mathbb{R}^{n_o \times n_e}$ at each iteration can be large with the large size of observational dataset n_o . Additionally, optimizing the whole matrix at each iteration is also not suitable for a deep learning framework that is based on mini-batch training. To tackle this challenge, inspired by [59], we propose a mini-batch OT based on a randomly sub-sampled observational dataset and provide its theoretical analysis as follows:

Definition 1. Consider two empirical distributions α and β with n and m units, we assume the batch size b of the first distribution α satisfy $b \mid n$ and let $k = n/b$ be the number of batches. Let \mathcal{B}_i be index set of the i -th batch in α and the corresponding empirical distribution is $\alpha_{\mathcal{B}_i}$, then the mini-batch OT problem is defined as:

$$m\text{-}OT(\alpha, \beta) = \frac{1}{k} \sum_{i=1}^k OT(\alpha_{\mathcal{B}_i}, \beta). \quad (5)$$

Theorem 3. Let γ_i be the optimal transport probability matrix of the i -th batch OT problem of $m\text{-}OT(P(\mathbf{S}, \mathbf{X}, A|G = o), P(\mathbf{S}, \mathbf{X}, A|G = e))$, i.e., $OT(P_{\mathcal{B}_i}(\mathbf{S}, \mathbf{X}, A|G = o), P(\mathbf{S}, \mathbf{X}, A|G = e))$. With extending γ_i to a $n_o \times n_e$ matrix Γ_i that pads zero entries to the row whose index does not belong to \mathcal{B}_i , we have:

$$\frac{1}{k} \sum_{i=1}^k \Gamma_i \in \Pi(P(\mathbf{S}, \mathbf{X}, A|G = o), P(\mathbf{S}, \mathbf{X}, A|G = e)), \quad (6)$$

and

$$OT(P(\mathbf{S}, \mathbf{X}, A|G = o), P(\mathbf{S}, \mathbf{X}, A|G = e)) \leq m\text{-}OT(P(\mathbf{S}, \mathbf{X}, A|G = o), P(\mathbf{S}, \mathbf{X}, A|G = e)). \quad (7)$$

The proof is in Appendix A.4. Theorem 3 implies that the OT distance of the joint distribution $P(\mathbf{S}, \mathbf{X}, A)$ between observational and experimental datasets is upper-bounded by its corresponding $m\text{-}OT$ problem. Solving the $m\text{-}OT$ problem not only significantly reduces the high optimization cost, but also allows us to embed the OT distance into the deep learning framework, where only batch observational units and full experimental units are considered at each training iteration.

Conclusion We have overcome two challenges about the conditional OT distance and high computational cost via theorem 2 and theorem 3 respectively. Combining these two theorems, we could learn the weights \mathbf{w}_o by minimizing $m\text{-}OT(P(\mathbf{S}, \mathbf{X}, A|G = o), P(\mathbf{S}, \mathbf{X}, A|G = e))$, which is upper bound of the original $OT_{\mathbf{x},a}^{con}$. As a result, our estimated weights \mathbf{w}_o could achieve Proposition 1 approximately, which leads to the identification of HDRC according to Theorem 1.

4.2 Generalization Bound on Long-term HDRC Estimation Error

Ideally, learning the OT-induced weights \mathbf{w}_o removes the unobserved confounding and makes HDRC identifiable. However, in estimating long-term HDRC, the counterfactual prediction error is still large. The reason is that the regression can only be trained with one of the counterfactual outcomes (factual outcomes) while the counterfactual outcomes are infinite due to the continuous treatment and the confounding bias exists since $\mathbf{X} \not\perp A$. To address it, in this section, we derive the generalization bound on the counterfactual prediction error, based on the OT-based reweighted distribution of the observational dataset.

We first define some notations used in the following discussion. Let $\phi : \mathcal{X} \rightarrow \mathcal{Z}$ be a representation function with inverse $\psi : \mathcal{Z} \rightarrow \mathcal{X}$, where \mathcal{Z} is the representation space. Let $g : \mathcal{Z} \times \mathcal{A} \rightarrow \mathcal{S}$ and $h : \mathcal{Z} \times \mathcal{A} \times \mathcal{S} \rightarrow \mathcal{Y}$ be the hypotheses that predict the short and long-term outcomes, respectively. Note that the HDRC estimator aims to predict potential long-term outcome $Y(a)$ for all possible treatments a on each unit \mathbf{x} , which requires that we could already predict the potential short-term outcomes $\mathbf{S}(a)$ accurately. As a result, we define the combined loss for learning these two hypotheses g, h as $\ell_{\phi,g,h}(\mathbf{x}, a) = \ell_{\phi,g}^s(\mathbf{x}, a) + \ell_{\phi,h}^y(\mathbf{x}, a)$, where $\ell_{\phi,g}^s(\mathbf{x}, a) = \int_{\mathcal{S}} L(s(a), g(\phi(\mathbf{x}), a))P(s(a)|\mathbf{x})ds(a)$ and $\ell_{\phi,h}^y(\mathbf{x}, a) = \int_{\mathcal{S} \times \mathcal{Y}} L(y(a), h(\phi(\mathbf{x}), a, s(a)))P(y(a), s(a)|\mathbf{x})ds(a)dy(a)$ ($L(\cdot, \cdot)$ is the error function). Therefore, the ideal prediction error over all treatment a for unit \mathbf{x} can be defined as $\mathcal{E}(\mathbf{x}) = \mathbb{E}_{a \sim P(A)}[\ell_{\phi,g,h}(\mathbf{x}, a)]$, and then the target of counterfactual prediction is minimizing $\mathcal{E}_{cf} = \mathbb{E}_{\mathbf{x} \sim P(\mathbf{X})}[\mathcal{E}(\mathbf{x})]$.

However, \mathcal{E}_{cf} is practically incomputable, because the actual datasets we access lack the counterfactual outcomes. As a result, we can only obtain the prediction error on the reweighted factual distribution as $\mathcal{E}_f^{\mathbf{w}_o} = \mathbb{E}_{\mathbf{x}, a \sim P^{\mathbf{w}_o}(\mathbf{X}, A)}[\ell_{\phi,g,h}(\mathbf{x}, a)]$. Next, following [46, 6], we derive a generalization bound to bridge a connection between \mathcal{E}_{cf} and $\mathcal{E}_f^{\mathbf{w}_o}$ in the long-term HDRC scenario:

Theorem 4. Assuming a family \mathcal{M} of function $m : \mathcal{Z} \times \mathcal{A} \rightarrow \mathbb{R}$, and there exists a constant $B_\phi > 0$ such that $\frac{1}{B_\phi} \cdot \ell_{\phi,g,h}(\mathbf{x}, a) \in \mathcal{M}$, then we have:

$$\mathcal{E}_{cf} \leq \mathcal{E}_f^{\mathbf{w}_o} + IPM_{\mathcal{M}}(P(\mathbf{Z})P(A), \mathbf{w}_o \cdot P(\mathbf{Z}, A)), \quad (8)$$

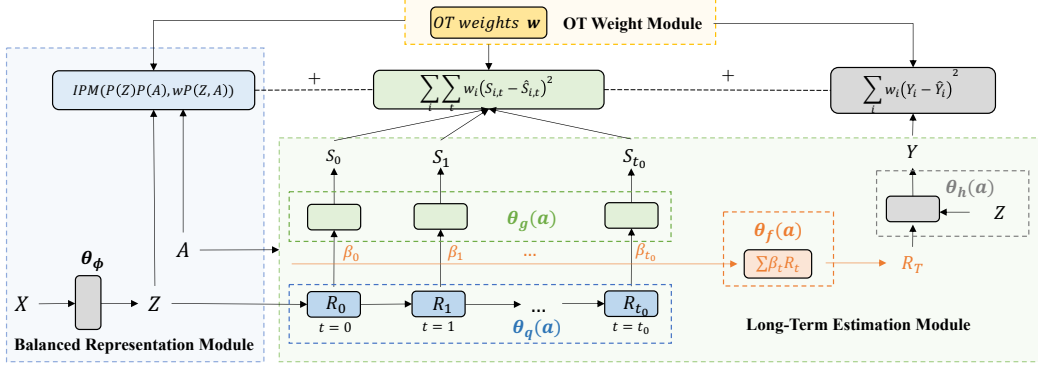


Figure 2: Model architecture of the proposed LEARN.

where $IPM_{\mathcal{M}}(p, q) = \sup_{m \in \mathcal{M}} |\int_{\mathcal{X}} g(x)(p(x) - q(x))dx|$ is integral probability metric for a chosen \mathcal{M} , $P(\mathbf{Z})$ and $P(\mathbf{Z}, A)$ are distributions induced by the map ϕ from $P(\mathbf{X})$ and $P(\mathbf{X}, A)$.

The proof is given in Appendix A.5. Theorem 4 states that the counterfactual error \mathcal{E}_{cf} is upper-bounded by the factual error $\mathcal{E}_f^{\text{wo}}$ plus an IPM term that measures the dependence between treatment A and covariates \mathbf{X} . The theorem inspires a classical balanced representation method based on deep learning [46], which handles the observed confounding bias by learning the balanced representation $\mathbf{Z} = \phi(\mathbf{X})$ that is independent of treatment A , i.e., $\mathbf{Z} \perp\!\!\!\perp A$.

5 Model Architecture

We have presented the theoretical results of our method, which handle the unobserved and observed confounders by reweighting and representation learning, respectively. In this section, we summarize the model architecture of LEARN inspired by these theoretical results. As shown in Fig. 2, LEARN can be divided into three modules: OT weight module, balanced representation module and long-term estimation module.

OT Weight Module This module is designed based on Theorems 2 and 3, which aims to estimate weights \mathbf{w}_o for removing the unobserved confounding bias. In order to embed the mini-batch OT problem $m\text{-}OT(\alpha, \beta)$ into the deep learning framework, following [59], we approximate it by solving $OT(\alpha_{\mathcal{B}}, \beta)$ over each mini-batch. As a result, we learn the weights $\mathbf{w}_{o,\mathcal{B}} = \{w_{o,1}, w_{o,2}, \dots, w_{o,b}\}$ by minimizing $OT(P_{\mathcal{B}}(\mathbf{S}, \mathbf{X}, A|G = o), P(\mathbf{S}, \mathbf{X}, A|G = e))$ between the batch observational dataset and full experimental dataset at each iteration. However, optimizing the OT problem directly usually induces a sparse solution, which means only a limited number of observational units are transported, suffering from low data efficiency [8, 54]. Motivated by [58], we apply a negative entropy regularization on the marginal distributions $\mathbf{w}_{o,\mathcal{B}}$, i.e., $\Omega(\mathbf{w}_{o,\mathcal{B}}) = \sum_{j=1}^b w_{o,j}(\log w_{o,j} - 1)$, to encourage more observational samples to be transported, and also avoid the heavy computation of solving the linear programming problem [16]. Finally, we learning weights $\mathbf{w}_{o,\mathcal{B}}$ as follows:

$$\begin{aligned} & \min_{\mathbf{w}_{o,\mathcal{B}}} \min_{\gamma \in \Pi(\alpha_{\mathcal{B}}, \beta)} \langle \gamma, \mathbf{C} \rangle + \lambda_e \Omega(\gamma), \\ & \text{s.t. } \Pi(\alpha_{\mathcal{B}}, \beta) = \{\gamma \in \mathbb{R}^{b \times n_e} | \gamma \mathbf{1}_{n_e} = \mathbf{w}_{o,\mathcal{B}}, \gamma^T \mathbf{1}_b = \boldsymbol{\mu}, \gamma_{ij} \in [0, 1]\}, \end{aligned} \quad (9)$$

where λ_e is the hyperparameter for the entropic constraint. We construct the cost matrix \mathbf{C} reflecting the transport cost between $P_{\mathcal{B}}(\mathbf{S}, \mathbf{X}, A|G = o)$ and $P(\mathbf{S}, \mathbf{X}, A|G = e)$ as $C_{ij} = \beta_r d(\bar{\mathbf{r}}_i, \bar{\mathbf{r}}_j) + \beta_x d(\mathbf{x}_i, \mathbf{x}_j) + \beta_a d(a_i, a_j)$, where $\beta_r, \beta_x, \beta_a$ are the hyperparameters, $d(\cdot, \cdot)$ is the euclidean distance, and the distance of short-term outcomes is calculated from the mean embedding of RNN in the long-term estimation module as $\bar{\mathbf{r}} = \frac{1}{t_0} \sum_{t=1}^{t_0} \mathbf{r}_t$. As a result, we need to pre-train the model firstly to ensure that the RNN's embedding is meaningful.

Following [58], we develop a projected mirror descent [40, 43] to solve the problem (9), which firstly performs proximal gradient descent with the Bregman divergence [5], and then obtains a feasible solution in the set $\Pi(\alpha_{\mathcal{B}}, \beta)$ by projection. The details can be found in Appendix B.

Balanced Representation Module This module is designed based on Theorem 4, which aims to correct the observed confounding bias at each iteration through learning the balanced representation \mathbf{Z} via minimizing $IPM(P(\mathbf{Z})P(A), \mathbf{w}_{o,\mathcal{B}}P(\mathbf{Z}, A))$. In practice, we use the Wasserstein distance

[53] as the implementation of the IPM term. To calculate it, we simulate samples standing for the product of marginal distributions $P(\mathbf{Z})P(A)$ by randomly permuting the observed treatment A , and the original samples are drawn from the joint distribution $P(\mathbf{Z}, A)$.

Long-Term Estimation Module This module aims to estimate the potential long-term outcome $Y(a)$ based on potential short-term outcomes $\mathbf{S}(a)$ for different units, and we follow LTEE [12] to model the relationship between the short and long-term outcomes. Specifically, the balanced representations \mathbf{Z} are firstly fed into the RNN $q(\cdot)$ to obtain the short-term representations \mathbf{R}_t at each timestep t , which is then used to predict the corresponding short-term outcome \hat{S}_t with a shared MLP $g(\cdot)$. After that, we leverage the attention mechanism $f(\cdot)$ [4] to construct the long-term representation \mathbf{R}_T from $\{\mathbf{R}_1, \mathbf{R}_2, \dots, \mathbf{R}_{t_0}\}$, and then predict the long-term outcome \hat{Y}_T through an MLP $h(\cdot)$.

Different from the original LTEE which only works with binary treatment, we follow the varying coefficient networks [41] to extend this module to a continuous treatment scenario. In particular, we use splines to model the parameters $\theta(a)$ of the above four network structures $q(\cdot), g(\cdot), f(\cdot), h(\cdot)$ as $\theta(a) = \sum_{l=1}^L \alpha_l \phi_l(a)$, where ϕ_l is the polynomial basis function and α_l is the coefficient. As a result, the influence of the treatment information is not lost in high-dimensional representations, which in practice has been shown to lead to better performance.

The training loss at each iteration of the balanced representation module and long-term estimation module is:

$$\begin{aligned} \mathcal{L}_\theta = & \frac{1}{b} \sum_{i=1}^b w_{o,i} (Y_i - \hat{Y}_i)^2 + \frac{\lambda_o}{b} \sum_{i=1}^b \sum_{t=1}^{t_0} w_{o,i} (S_{i,t} - \hat{S}_{i,t})^2 + \frac{1 - \lambda_o}{n_e} \sum_{i=1}^{n_e} \sum_{t=1}^{t_0} (S_{i,t} - \hat{S}_{i,t})^2 \\ & + \lambda_b IPM(\{\phi(\mathbf{X}_i), \tilde{A}_i\}_{i=0}^b, \{w_{o,i}\phi(\mathbf{X}_i), w_{o,i}A_i\}_{i=0}^b), \end{aligned} \quad (10)$$

where $\theta = \{\theta_\phi, \theta_q(a), \theta_g(a), \theta_f(a), \theta_h(a)\}$, λ_b means the strength of IPM, and \tilde{A}_i is the samples obtained by randomly permuting original treatment samples A_i . To make full use of the datasets, in addition to the observational dataset, we also train the model based on the prediction error of the short-term outcomes on the experimental dataset, and use λ_o to control its strength. We also provide more detail and the pseudocode of LEARN in Appendix D.

6 Experiments

6.1 Experimental Setup

Dataset Generation Since the true HDRC is unavailable for real-world datasets, following existing literature [45, 7, 41, 56, 34], we use five synthetic datasets with varying $\beta_U \in \{1, 1.25, 1.5, 1.75, 2\}$ that denotes different strengths of unobserved confounding bias, and two semi-synthetic datasets, News [45] and TCGA [57], to demonstrate the effectiveness of our model. The details of the dataset generation can be found in Appendix E.1.

Baselines and Metrics We first compare our model LEARN with the following baselines designed for continuous treatment, including DRNet [45], VCNet [41], SCIGAN [7], ADMIT [56] and ACFR [34]. Besides, since there is a lack of work on estimating long-term HDRC, we modify LTEE [12] into a baseline suitable for continuous treatment by introducing the varying coefficient structure, denoted as LTEE(VCNet). Moreover, to verify the effectiveness of the OT weight module and IPM term, we implement two variants of our model: LEARN(None) is the variant without any module to correct confounding bias, and LEARN(IPM) is the variant with only the IPM term to correct observed confounding bias without considering the unobserved one. For metrics, we first split the observational dataset with a 6/2/2 ratio into training, validation and test sets, and we report the mean integrated square error (MISE) and the deviations (std) of HDRC estimation on the test set by performing 10 replications: $MISE = \frac{1}{s} \sum_{i=1}^s \int_{a_1}^{a_2} (Y(a) - \hat{Y}(a))^2 da$, where s is the test sample size and $[a_1, a_2]$ is the sampling interval of treatment values.

6.2 Result and Analysis

Overall Performance In Table 1, we compare our model with baselines on both synthetic and semi-synthetic datasets, and the main observations are as follows. Firstly, compared with the baselines only designed for continuous treatment, LEARN obtains the highest accuracy in estimating the

Table 1: Results of HDRC estimation on five synthetic and two semi-synthetic datasets. The MISE is reported as Mean \pm Std. The best-performing method is bolded.

Dataset	Synthetic					News	TCGA
	$\beta_U = 1$	$\beta_U = 1.25$	$\beta_U = 1.5$	$\beta_U = 1.75$	$\beta_U = 2$		
DRNet	66.77 \pm 13.26	69.23 \pm 13.64	72.92 \pm 13.73	78.43 \pm 14.68	86.67 \pm 18.61	26.47 \pm 10.07	0.788 \pm 0.781
SCIGAN	75.92 \pm 14.17	78.29 \pm 12.85	82.03 \pm 14.13	87.82 \pm 14.88	94.64 \pm 15.61	26.61 \pm 10.09	1.747 \pm 1.823
VCNet	63.31 \pm 12.77	65.78 \pm 12.64	69.55 \pm 12.39	74.19 \pm 12.62	79.86 \pm 13.00	9.42 \pm 3.13	0.187 \pm 0.146
ADMIT	62.91 \pm 12.13	66.65 \pm 13.69	70.24 \pm 13.54	74.59 \pm 12.92	81.15 \pm 14.18	16.58 \pm 8.72	0.143 \pm 0.081
ACRF	64.64 \pm 8.33	67.38 \pm 8.14	71.30 \pm 8.28	76.17 \pm 9.52	82.97 \pm 11.29	22.81 \pm 9.39	0.465 \pm 0.379
LTEE(VCNet)	61.79 \pm 12.48	63.98 \pm 12.90	67.55 \pm 12.03	73.34 \pm 12.67	78.79 \pm 13.33	10.11 \pm 2.76	0.137 \pm 0.097
LEARN(None)	62.49 \pm 12.24	64.27 \pm 12.69	68.08 \pm 12.09	74.08 \pm 12.95	79.99 \pm 12.82	8.86 \pm 3.18	0.145 \pm 0.111
LEARN(IPM)	61.75 \pm 12.64	63.90 \pm 12.13	67.41 \pm 12.01	73.05 \pm 12.82	78.37 \pm 13.00	8.76 \pm 3.14	0.141 \pm 0.106
LEARN	60.57 \pm 11.98	62.74 \pm 12.24	66.02 \pm 11.59	71.00 \pm 12.17	76.76 \pm 12.90	8.31 \pm 2.90	0.131 \pm 0.101

HRDC in all datasets. The accuracy improvement comes from the designed long-term estimation module, employing the attention mechanism to capture the relationship between the short-term and long-term outcomes, and this is also the reason why LTEE(VCNet) performs relatively well. Secondly, we observe that LEARN(IPM) consistently outperforms LEARN(None), indicating that learning balanced representations through minimizing the IPM term indeed reduces the observed confounding bias, resulting in smaller MISE. Finally, LEARN achieves superior performance compared with LEARN(IPM), and the improvement increases with the increase of β_U , which reflects the necessity of considering the unobserved confounders. The improvement verifies the effectiveness of the reweighting based on our designed OT weight module.

Performance of Confounding Bias Correction In Table 2, we evaluate the effectiveness of our design modules in correcting confounding bias using the synthetic dataset ($\beta_U = 1$), including the observed and unobserved ones. Regarding observed confounding bias, it arises from the correlation between \mathbf{X} and A , and we verify the effectiveness of a balanced representation module in correcting such a bias. We use the Hilbert-Schmidt Independence Criterion (HSIC[24]) to measure the independence between the learned $\mathbf{Z} = \phi(\mathbf{X})$ and A . The result reveals an 86.11% reduction in the correlation between \mathbf{X} and A , indicating the remarkable decrease in the observed confounding bias, which is also consistent with the comparison results between LEARN(None) and LEARN(IPM) in Table 1.

Regarding unobserved confounders, our designed OT weight module handles them by reweighting. The effectiveness of this module is evaluated using the Hilbert-Schmidt Conditional Independence Criterion (HSCONIC, [20, 47]), which measures the degree to which reweighting makes the unconfoundedness in the observational dataset satisfied, i.e., $A \perp\!\!\!\perp \{Y(a), \mathbf{S}(a)\} | \mathbf{X}, G = o$. The result indicates a substantial decrease in the correlations between $\mathbf{S}(a)$ and A , as well as between $Y(a)$ and A given \mathbf{X} , by 61.55% and 66.17% respectively, suggesting an enhanced satisfaction of the unconfoundedness assumption after reweighting, consistent with the comparison results between LEARN(IPM) and LEARN in Table 1.

Table 2: Results of the model performance in reducing observed and unobserved confounding bias, using HSIC as a metric of correlation.

	Observed	Unobserved	
	HSIC(\mathbf{X}, A)	HSCONIC($\mathbf{S}(a), A \mathbf{X}$)	HSCONIC($Y(a), A \mathbf{X}$)
Reduce ratio	86.11%	61.55%	66.17%

Impact of Sample Size on Experimental Dataset Since our proposed LEARN relies on the data combination with an experimental dataset, we exploit the impact of the experimental dataset’s sample size on MISE using the synthetic dataset ($\beta_U = 1$) and report the results in Table 3. As expected, the MISE decreases as the sample size increases, attributable to the larger experimental dataset providing a more reliable distribution for aligning the observational dataset, which allows us to learn more effective weights for eliminating unobserved confounding bias.

Table 3: The impact of experimental dataset’s sample size on the MISE of HDRC estimation.

Number	100	250	500	1000	2000
MISE	61.24 \pm 11.74	60.95 \pm 11.53	60.57 \pm 11.98	59.46 \pm 11.29	59.02 \pm 11.39

Hyperparameter Sensitivity Study We investigate the role of three hyperparameters in our model: $\lambda_o, \lambda_b, \lambda_e$. The details can be found in Appendix E.2.

7 Conclusion

In this paper, we provide a practical solution to estimate the long-term HDRC with unobserved confounders on observational data via data combination, which is not well-studied in existing work. Specifically, to remove unobserved confounders and make long-term HDRC identifiable, we first propose a novel weighting schema aligning the conditional distribution of short-term outcomes between observational and experimental groups. We solve the reweighting problem under an optimal transport framework, showing that the conditional distribution discrepancy can be bounded by mini-batch joint distribution discrepancy, which is computationally efficient. Further, to handle the observed confounders, we derive a generalization bound on the counterfactual outcome regression error based on the OT-induced reweighted distribution. Building upon the above theoretical results, we develop our model LEARN to estimate long-term HDRC accurately. Extensive experimental results verify the correctness of our theory and the effectiveness of LEARN.

Acknowledgements

This research was supported in part by National Key R&D Program of China (2021ZD0111501), National Science Fund for Excellent Young Scholars (62122022), Natural Science Foundation of China (62206064, 62206061), Guangdong Basic and Applied Basic Research Foundation (2024A1515011901), Guangzhou Basic and Applied Basic Research Foundation (2023A04J1700), and CCF-DiDi GAIA Collaborative Research Funds (CCF-DiDi GAIA 202311).

References

- [1] M. Arjovsky, S. Chintala, and L. Bottou. Wasserstein generative adversarial networks. In *International conference on machine learning*, pages 214–223. PMLR, 2017.
- [2] S. Athey, R. Chetty, G. W. Imbens, and H. Kang. The surrogate index: Combining short-term proxies to estimate long-term treatment effects more rapidly and precisely. Technical report, National Bureau of Economic Research, 2019.
- [3] S. Athey, R. Chetty, and G. Imbens. Combining experimental and observational data to estimate treatment effects on long term outcomes. *arXiv preprint arXiv:2006.09676*, 2020.
- [4] D. Bahdanau, K. Cho, and Y. Bengio. Neural machine translation by jointly learning to align and translate. *arXiv preprint arXiv:1409.0473*, 2014.
- [5] A. Banerjee, S. Merugu, I. S. Dhillon, J. Ghosh, and J. Lafferty. Clustering with bregman divergences. *Journal of machine learning research*, 6(10), 2005.
- [6] A. Bellot, A. Dhir, and G. Prando. Generalization bounds and algorithms for estimating conditional average treatment effect of dosage. *arXiv preprint arXiv:2205.14692*, 2022.
- [7] I. Bica, J. Jordon, and M. van der Schaar. Estimating the effects of continuous-valued interventions using generative adversarial networks. *Advances in Neural Information Processing Systems*, 33:16434–16445, 2020.
- [8] M. Blondel, V. Seguy, and A. Rolet. Smooth and sparse optimal transport. In *International conference on artificial intelligence and statistics*, pages 880–889. PMLR, 2018.
- [9] R. Cai, W. Chen, Z. Yang, S. Wan, C. Zheng, X. Yang, and J. Guo. Long-term causal effects estimation via latent surrogates representation learning. *Neural Networks*, page 106336, 2024.
- [10] W. Chang, Y. Shi, H. Tuan, and J. Wang. Unified optimal transport framework for universal domain adaptation. *Advances in Neural Information Processing Systems*, 35:29512–29524, 2022.
- [11] J. Chen and D. M. Ritzwoller. Semiparametric estimation of long-term treatment effects. *Journal of Econometrics*, 237(2):105545, 2023.

- [12] L. Cheng, R. Guo, and H. Liu. Long-term effect estimation with surrogate representation. In *Proceedings of the 14th ACM International Conference on Web Search and Data Mining*, pages 274–282, 2021.
- [13] R. Chetty, J. N. Friedman, N. Hilger, E. Saez, D. W. Schanzenbach, and D. Yagan. How does your kindergarten classroom affect your earnings? evidence from project star. *The Quarterly journal of economics*, 126(4):1593–1660, 2011.
- [14] N. Courty, R. Flamary, D. Tuia, and A. Rakotomamonjy. Optimal transport for domain adaptation. *IEEE transactions on pattern analysis and machine intelligence*, 39(9):1853–1865, 2016.
- [15] N. Courty, R. Flamary, A. Habrard, and A. Rakotomamonjy. Joint distribution optimal transportation for domain adaptation. *Advances in neural information processing systems*, 30, 2017.
- [16] M. Cuturi. Sinkhorn distances: Lightspeed computation of optimal transport. In *Annual Conference on Neural Information Processing Systems*, pages 2292–2300, 2013.
- [17] B. B. Damodaran, B. Kellenberger, R. Flamary, D. Tuia, and N. Courty. Deepjdot: Deep joint distribution optimal transport for unsupervised domain adaptation. In *Proceedings of the European conference on computer vision (ECCV)*, pages 447–463, 2018.
- [18] E. Dunipace. Optimal transport weights for causal inference. *arXiv preprint arXiv:2109.01991*, 2021.
- [19] T. R. Fleming, R. L. Prentice, M. S. Pepe, and D. Glidden. Surrogate and auxiliary endpoints in clinical trials, with potential applications in cancer and aids research. *Statistics in medicine*, 13(9):955–968, 1994.
- [20] K. Fukumizu, A. Gretton, X. Sun, and B. Schölkopf. Kernel measures of conditional dependence. *Advances in neural information processing systems*, 20, 2007.
- [21] J. Gao, H. Zhao, Z. Li, and D. Guo. Enhancing minority classes by mixing: An adaptive optimal transport approach for long-tailed classification. *Advances in Neural Information Processing Systems*, 36, 2024.
- [22] A. Genevay, G. Peyré, and M. Cuturi. Learning generative models with sinkhorn divergences. In *International Conference on Artificial Intelligence and Statistics*, pages 1608–1617. PMLR, 2018.
- [23] A. Ghassami, A. Yang, D. Richardson, I. Shpitser, and E. T. Tchetgen. Combining experimental and observational data for identification and estimation of long-term causal effects. *arXiv preprint arXiv:2201.10743*, 2022.
- [24] A. Gretton, O. Bousquet, A. Smola, and B. Schölkopf. Measuring statistical dependence with hilbert-schmidt norms. In *International conference on algorithmic learning theory*, pages 63–77. Springer, 2005.
- [25] F. Gunsilius and Y. Xu. Matching for causal effects via multimarginal unbalanced optimal transport. *arXiv preprint arXiv:2112.04398*, 2021.
- [26] D. Guo, Z. Li, H. Zhao, M. Zhou, H. Zha, et al. Learning to re-weight examples with optimal transport for imbalanced classification. *Advances in Neural Information Processing Systems*, 35:25517–25530, 2022.
- [27] H. Hohnhold, D. O’Brien, and D. Tang. Focusing on the long-term: It’s good for users and business. In *Proceedings of the 21th ACM SIGKDD International Conference on Knowledge Discovery and Data Mining*, pages 1849–1858, 2015.
- [28] W. Hu, X. Zhou, and P. Wu. Identification and estimation of treatment effects on long-term outcomes in clinical trials with external observational data. *Statistica Sinica*. doi: 10.5705/ss.202023.0006.

- [29] V. Huynh and D. Phung. Optimal transport for deep generative models: State of the art and research challenges. In *International Joint Conference on Artificial Intelligence 2021*, pages 4450–4457. Association for the Advancement of Artificial Intelligence (AAAI), 2021.
- [30] G. Imbens, N. Kallus, X. Mao, and Y. Wang. Long-term causal inference under persistent confounding via data combination. *arXiv preprint arXiv:2202.07234*, 2022.
- [31] G. W. Imbens. The role of the propensity score in estimating dose-response functions. *Biometrika*, 87(3):706–710, 2000.
- [32] N. Kallus and X. Mao. On the role of surrogates in the efficient estimation of treatment effects with limited outcome data. *arXiv preprint arXiv:2003.12408*, 2020.
- [33] L. V. Kantorovich. On the translocation of masses. *Journal of mathematical sciences*, 133(4): 1381–1382, 2006.
- [34] A. Kazemi and M. Ester. Adversarially balanced representation for continuous treatment effect estimation. In *Proceedings of the AAAI Conference on Artificial Intelligence*, volume 38, pages 13085–13093, 2024.
- [35] E. H. Kennedy, Z. Ma, M. D. McHugh, and D. S. Small. Non-parametric methods for doubly robust estimation of continuous treatment effects. *Journal of the Royal Statistical Society Series B: Statistical Methodology*, 79(4):1229–1245, 2017.
- [36] D. P. Kingma and J. Ba. Adam: A method for stochastic optimization. *arXiv preprint arXiv:1412.6980*, 2014.
- [37] A. Korotin, V. Egiazarian, A. Asadulaev, A. Safin, and E. Burnaev. Wasserstein-2 generative networks. *arXiv preprint arXiv:1909.13082*, 2019.
- [38] M. Li, D. Wang, X. Liu, Z. Zeng, R. Lu, B. Chen, and M. Zhou. Patchct: Aligning patch set and label set with conditional transport for multi-label image classification. In *Proceedings of the IEEE/CVF International Conference on Computer Vision*, pages 15348–15358, 2023.
- [39] Q. Li, Z. Wang, S. Liu, G. Li, and G. Xu. Causal optimal transport for treatment effect estimation. *IEEE transactions on neural networks and learning systems*, 34(8):4083–4095, 2021.
- [40] A. S. Nemirovskij and D. B. Yudin. Problem complexity and method efficiency in optimization. 1983.
- [41] L. Nie, M. Ye, qiang liu, and D. Nicolae. Varying coefficient neural network with functional targeted regularization for estimating continuous treatment effects. In *International Conference on Learning Representations*, 2021. URL <https://openreview.net/forum?id=RmB-88r9dL>.
- [42] A. B. Owen. Monte carlo theory, methods and examples, 2013.
- [43] G. Raskutti and S. Mukherjee. The information geometry of mirror descent. *IEEE Transactions on Information Theory*, 61(3):1451–1457, 2015.
- [44] D. B. Rubin. Estimating causal effects of treatments in randomized and nonrandomized studies. *Journal of educational Psychology*, 66(5):688, 1974.
- [45] P. Schwab, L. Linhardt, S. Bauer, J. M. Buhmann, and W. Karlen. Learning counterfactual representations for estimating individual dose-response curves. In *Proceedings of the AAAI Conference on Artificial Intelligence*, volume 34, pages 5612–5619, 2020.
- [46] U. Shalit, F. D. Johansson, and D. Sontag. Estimating individual treatment effect: generalization bounds and algorithms. In *International conference on machine learning*, pages 3076–3085. PMLR, 2017.
- [47] X. Sun, D. Janzing, B. Schölkopf, and K. Fukumizu. A kernel-based causal learning algorithm. In *Proceedings of the 24th international conference on Machine learning*, pages 855–862, 2007.

- [48] L. Tian, J. Feng, X. Chai, W. Chen, L. Wang, X. Liu, and B. Chen. Prototypes-oriented transductive few-shot learning with conditional transport. In *Proceedings of the IEEE/CVF International Conference on Computer Vision*, pages 16317–16326, 2023.
- [49] S. Tübbicke. Entropy balancing for continuous treatments. *Journal of Econometric Methods*, 11(1):71–89, 2022.
- [50] G. Van Goffrier, L. Maystre, and C. M. Gilligan-Lee. Estimating long-term causal effects from short-term experiments and long-term observational data with unobserved confounding. In *Conference on Causal Learning and Reasoning*, pages 791–813. PMLR, 2023.
- [51] B. G. Vegetabile, B. A. Griffin, D. L. Coffman, M. Cefalu, M. W. Robbins, and D. F. McCaffrey. Nonparametric estimation of population average dose-response curves using entropy balancing weights for continuous exposures. *Health Services and Outcomes Research Methodology*, 21: 69–110, 2021.
- [52] C. Villani. *Topics in optimal transportation*, volume 58. American Mathematical Soc., 2021.
- [53] C. Villani et al. *Optimal transport: old and new*, volume 338. Springer, 2009.
- [54] C. Vincent-Cuaz, R. Flamary, M. Corneli, T. Vayer, and N. Courty. Semi-relaxed gromov wasserstein divergence with applications on graphs. In *International Conference on Learning Representations*, 2022.
- [55] H. Wang, J. Fan, Z. Chen, H. Li, W. Liu, T. Liu, Q. Dai, Y. Wang, Z. Dong, and R. Tang. Optimal transport for treatment effect estimation. *Advances in Neural Information Processing Systems*, 36, 2024.
- [56] X. Wang, S. Lyu, X. Wu, T. Wu, and H. Chen. Generalization bounds for estimating causal effects of continuous treatments. *Advances in Neural Information Processing Systems*, 35: 8605–8617, 2022.
- [57] J. N. Weinstein, E. A. Collisson, G. B. Mills, K. R. Shaw, B. A. Ozenberger, K. Ellrott, I. Shmulevich, C. Sander, and J. M. Stuart. The cancer genome atlas pan-cancer analysis project. *Nature genetics*, 45(10):1113–1120, 2013.
- [58] Y. Yan, Z. Yang, W. Chen, R. Cai, Z. Hao, and M. K.-P. Ng. Exploiting geometry for treatment effect estimation via optimal transport. In *Proceedings of the AAAI Conference on Artificial Intelligence*, volume 38, pages 16290–16298, 2024.
- [59] Y. Yang, X. Gu, and J. Sun. Prototypical partial optimal transport for universal domain adaptation. In *Proceedings of the AAAI Conference on Artificial Intelligence*, volume 37, pages 10852–10860, 2023.
- [60] Z. Zeng, D. Arbour, A. Feller, R. Addanki, R. Rossi, R. Sinha, and E. H. Kennedy. Continuous treatment effects with surrogate outcomes. *arXiv preprint arXiv:2402.00168*, 2024.
- [61] Y. Zhu, D. L. Coffman, and D. Ghosh. A boosting algorithm for estimating generalized propensity scores with continuous treatments. *Journal of causal inference*, 3(1):25–40, 2015.

A Proof

A.1 Proof of Proposition 1

Proposition 1. *Under Assumptions 1, 2, 3, 4, and 5, given a set of weights $\mathbf{w} = \{\mathbf{w}_o, \boldsymbol{\mu}\}$ consisting of the learnable weights \mathbf{w}_o for observational units and uniform weights $\boldsymbol{\mu}$ for experimental units, which makes $\mathbf{w}P(\mathbf{S}, G|\mathbf{X}, A) = P^{\mathbf{w}}(\mathbf{S}, G|\mathbf{X}, A) = P^{\mathbf{w}}(\mathbf{S}|\mathbf{X}, A)P^{\mathbf{w}}(G|\mathbf{X}, A)$, i.e., $\mathbf{S} \perp\!\!\!\perp G|\mathbf{X}, A$, then $\mathbb{E}[\mathbf{S}(a)|\mathbf{X}, A = a, G = o] = \mathbb{E}[\mathbf{S}(a)|\mathbf{X}, G = o]$ holds on the weighted observational population.*

Proof. First, based on Assumption 1, we rewrite $P^{\mathbf{w}}(\mathbf{S}, G|\mathbf{X}, A) = P^{\mathbf{w}}(\mathbf{S}|\mathbf{X}, A)P^{\mathbf{w}}(G|\mathbf{X}, A)$ as $P^{\mathbf{w}}(\mathbf{S}(a), G|\mathbf{X}, A = a) = P^{\mathbf{w}}(\mathbf{S}(a)|\mathbf{X}, A = a)P^{\mathbf{w}}(G|\mathbf{X}, A = a)$. Based on chain rule, we have

$$P^{\mathbf{w}}(\mathbf{S}(a), G|\mathbf{X}, A = a) = P^{\mathbf{w}}(\mathbf{S}(a)|G, \mathbf{X}, A = a)P^{\mathbf{w}}(G|\mathbf{X}, A = a), \quad (1)$$

then we have

$$P^{\mathbf{w}}(\mathbf{S}(a)|\mathbf{X}, A = a) = P^{\mathbf{w}}(\mathbf{S}(a)|G, \mathbf{X}, A = a). \quad (2)$$

Note that, based on Eq. (2), we have

$$P^{\mathbf{w}}(\mathbf{S}(a)|\mathbf{X}, A = a) = P^{\mathbf{w}}(\mathbf{S}(a)|G, \mathbf{X}, A = a) = P^{\mathbf{w}}(\mathbf{S}(a)|G = e, \mathbf{X}, A = a), \quad (3)$$

and thus we have

$$P^{\mathbf{w}}(\mathbf{S}(a), G|\mathbf{X}, A = a) = P^{\mathbf{w}}(\mathbf{S}(a)|G = e, \mathbf{X}, A = a)P^{\mathbf{w}}(G|\mathbf{X}, A = a). \quad (4)$$

Based on Assumption 3, we have

$$P^{\mathbf{w}}(\mathbf{S}(a), G|\mathbf{X}, A = a) = P^{\mathbf{w}}(\mathbf{S}(a)|G = e, \mathbf{X})P^{\mathbf{w}}(G|\mathbf{X}, A = a). \quad (5)$$

Based on Assumption 4, we have

$$P^{\mathbf{w}}(\mathbf{S}(a), G|\mathbf{X}, A = a) = P^{\mathbf{w}}(\mathbf{S}(a)|G, \mathbf{X})P^{\mathbf{w}}(G|\mathbf{X}, A = a). \quad (6)$$

Hence, based on Eq. (1) and (6), we conclude

$$P^{\mathbf{w}}(\mathbf{S}(a)|A = a, G, \mathbf{X}) = P^{\mathbf{w}}(\mathbf{S}(a)|G, \mathbf{X}), \quad (7)$$

and thus $\mathbb{E}[\mathbf{S}(a)|A = a, G = o, \mathbf{X}] = \mathbb{E}[\mathbf{S}(a)|G = o, \mathbf{X}]$ hold.

□

A.2 Proof of Theorem 1

Theorem 1. *Suppose Assumptions in Proposition 1 hold, we have the unconfoundedness $\mathbb{E}[Y(a)|\mathbf{X}, A = a, G = o] = \mathbb{E}[Y(a)|\mathbf{X}, G = o]$, then the long-term HDRC can be identified.*

Proof. Firstly, we show that $\mathbb{E}[Y(a)|\mathbf{X}, A = a, G = o] = \mathbb{E}[Y(a)|\mathbf{X}, G = o]$ holds based on Proposition 1. Specifically,

$$\begin{aligned} P^{\mathbf{w}}(Y(a)|A = a, G = o, \mathbf{X}) &= \int P^{\mathbf{w}}(Y(a), \mathbf{S}(a)|A = a, G = o, \mathbf{X})d\mathbf{S}(a) \\ &= \int P^{\mathbf{w}}(Y(a)|\mathbf{S}(a), A = a, G = o, \mathbf{X})P^{\mathbf{w}}(\mathbf{S}(a)|A = a, G = o, \mathbf{X})d\mathbf{S}(a) \\ &= \int P^{\mathbf{w}}(Y(a)|\mathbf{S}(a), G = o, \mathbf{X})P^{\mathbf{w}}(\mathbf{S}(a)|G = o, \mathbf{X})d\mathbf{S}(a) \\ &= \int P^{\mathbf{w}}(Y(a), \mathbf{S}(a)|G = o, \mathbf{X})d\mathbf{S}(a) \\ &= P^{\mathbf{w}}(Y(a)|G = o, \mathbf{X}), \end{aligned} \quad (8)$$

where the second equality is based on the chain rule, the third equality is based on Assumption 5 and Eq. (7). Based on the above equality, we can directly conclude

$$\mathbb{E}[Y(a)|A = a, G = o, \mathbf{X}] = \mathbb{E}[Y(a)|G = o, \mathbf{X}]. \quad (9)$$

Then HDRC is identified:

$$\begin{aligned}
\mathbb{E}[Y(a)|X = x] &= \mathbb{E}[Y(a)|X = x, G = o] \\
&= \mathbb{E}[Y(a)|X = x, A = a, G = o] \\
&= \mathbb{E}[Y|X = x, A = a, G = o],
\end{aligned} \tag{10}$$

where the first equality is based on Assumption 4, the second equality is based on the result of Eq. (9), and the third equality is based on Assumption 1. \square

A.3 Proof of Theorem 2

We firstly define the empirical observational distribution $P(\mathbf{S}, \mathbf{X}, A|G = o)$ as $\alpha_{\mathbf{w}_o} = \sum_{i=1}^{n_o} w_{o,i} \delta(\mathbf{s}_i, \mathbf{x}_i, a_i)$, where \mathbf{w}_o is the to-be-learned weights, and we define the empirical experimental distribution $P(\mathbf{S}, \mathbf{X}, A|G = e)$ as $\beta = \sum_{i=1}^{n_e} \frac{1}{n_e} \delta(\mathbf{s}_i, \mathbf{x}_i, a_i)$. We also have the following lemma, which states the convergence of the importance sampling weights:

Lemma 1. *Under the positivity assumption, let the importance sampling weights as $\check{w}_{o,i}^* = \frac{dP(\mathbf{s}_i, \mathbf{x}_i, a_i|G=e)}{dP(\mathbf{s}_i, \mathbf{x}_i, a_i|G=o)}$ and the corresponding self-normalized weights as $w_{o,i}^* = \frac{\check{w}_{o,i}^*}{\sum_i \check{w}_{o,i}^*}$. Then we have $P(\lim_{n_o \rightarrow \infty} \alpha_{w_o^*} = \beta) = 1$.*

Based on Theorem 9.2 in [42], Lemma 1 is easy to establish by viewing $\delta(\mathbf{s}_i, \mathbf{x}_i, a_i)$ as the function of interest $f(\cdot)$ in the importance sampling.

Now we are ready to prove Theorem 2.

Theorem 2. *Assuming the cost matrix of the joint distribution $P(\mathbf{S}, \mathbf{X}, A)$ is separable, i.e., $C(\mathbf{s}, \mathbf{x}, a; \tilde{\mathbf{s}}, \tilde{\mathbf{x}}, \tilde{a}) = C(\mathbf{s}; \tilde{\mathbf{s}}) + C(\mathbf{x}; \tilde{\mathbf{x}}) + C(a; \tilde{a})$, we have:*

$$OT_{\mathbf{x},a}^{con} \leq OT(P(\mathbf{S}, \mathbf{X}, A|G = o), P(\mathbf{S}, \mathbf{X}, A|G = e)),$$

In addition, under the positivity assumption, we have $OT(P(\mathbf{S}, \mathbf{X}, A|G = o), P(\mathbf{S}, \mathbf{X}, A|G = e)) \rightarrow 0$ as $n_o \rightarrow \infty$, leading to $OT_{\mathbf{x},a}^{con} \rightarrow 0$.

Proof. With the separable assumption of the cost matrix, we abbreviate the cost matrix about the joint distribution $P(\mathbf{S}, \mathbf{X}, A)$ as $C_{\mathbf{s},\mathbf{x},a} = C_{\mathbf{s}} + C_{\mathbf{x}} + C_a$. Then for any $\Gamma_{\mathbf{s},\mathbf{x},a,\tilde{\mathbf{s}},\tilde{\mathbf{x}},\tilde{a}} \in \Pi(P(\mathbf{S}, \mathbf{X}, A|G = o), P(\mathbf{S}, \mathbf{X}, A|G = e))$, we have:

$$\begin{aligned}
OT(P(\mathbf{S}, \mathbf{X}, A|G = o), P(\mathbf{S}, \mathbf{X}, A|G = e)) &= \min_{\Gamma} \langle \Gamma_{\mathbf{s},\mathbf{x},a,\tilde{\mathbf{s}},\tilde{\mathbf{x}},\tilde{a}}, C_{\mathbf{s},\mathbf{x},a} \rangle \\
&= \min_{\Gamma} \langle \Gamma_{\mathbf{s},\mathbf{x},a,\tilde{\mathbf{s}},\tilde{\mathbf{x}},\tilde{a}}, C_{\mathbf{s}} + C_{\mathbf{x}} + C_a \rangle \\
&\geq \min_{\Gamma} \langle \Gamma_{\mathbf{s},\mathbf{x},a,\tilde{\mathbf{s}},\tilde{\mathbf{x}},\tilde{a}}, C_{\mathbf{s}} \rangle \\
&\geq \min_{\Gamma} \langle \Gamma_{\mathbf{s},\mathbf{x},a,\tilde{\mathbf{s}},\tilde{\mathbf{x}},\tilde{a}} \mathbb{I}(\mathbf{x} = \tilde{\mathbf{x}}, a = \tilde{a}), C_{\mathbf{s}} \rangle \\
&= \min_{\Gamma} \sum_{\mathbf{x},a,\tilde{\mathbf{x}},\tilde{a}} \mathbb{I}(\mathbf{x} = \tilde{\mathbf{x}}, a = \tilde{a}) \langle \Gamma_{\mathbf{s}|\mathbf{x},a,\tilde{\mathbf{s}}|\tilde{\mathbf{x}},\tilde{a}}, C_{\mathbf{s}} \rangle \\
&= \min_{\Gamma} \sum_{\mathbf{x},a} \langle \Gamma_{\mathbf{s}|\mathbf{x},a,\tilde{\mathbf{s}}|\mathbf{x},a}, C_{\mathbf{s}} \rangle \\
&= OT_{\mathbf{x},a}^{con}.
\end{aligned}$$

Next, we establish the convergence property. Recall that the definition of $\hat{\mathbf{w}}_o = \min_{\mathbf{w}_o} OT(P(\mathbf{S}, \mathbf{X}, A|G = o), P(\mathbf{S}, \mathbf{X}, A|G = e)) = \min_{\mathbf{w}_o} OT(\alpha_{\mathbf{w}_o}, \beta)$, we have $OT(\alpha_{\hat{\mathbf{w}}_o}, \beta) \leq OT(\alpha_{\mathbf{w}_o^*}, \beta)$. Based on Lemma 1, when $n_o \rightarrow \infty$, we could obtain:

$$\begin{aligned}
\alpha_{\mathbf{w}_o^*} \rightarrow \beta &\implies OT(\alpha_{\mathbf{w}_o^*}, \beta) \rightarrow 0 \\
&\implies OT(\alpha_{\hat{\mathbf{w}}_o}, \beta) \rightarrow 0,
\end{aligned}$$

which means that with the estimated weights $\hat{\mathbf{w}}_o$, we have $OT(P(\mathbf{S}, \mathbf{X}, A|G = o), P(\mathbf{S}, \mathbf{X}, A|G = e)) \rightarrow 0$. Therefore, we also have $OT_{\mathbf{x},a}^{con} \rightarrow 0$, since it is the lower bound of $OT(P(\mathbf{S}, \mathbf{X}, A|G = o), P(\mathbf{S}, \mathbf{X}, A|G = e))$. \square

A.4 Proof of Theorem 3

Theorem 3. Let γ_i be the optimal transport probability matrix of the i -th batch OT problem of m -OT($P(\mathbf{S}, \mathbf{X}, A|G = o), P(\mathbf{S}, \mathbf{X}, A|G = e)$), i.e., $OT(P_{\mathcal{B}_i}(\mathbf{S}, \mathbf{X}, A|G = o), P(\mathbf{S}, \mathbf{X}, A|G = e))$. We extend γ_i to a $n_o \times n_e$ matrix Γ_i that pads zero entries to the row whose index does not belong to \mathcal{B}_i , then we have:

$$\frac{1}{k} \sum_{i=1}^k \Gamma_i \in \Pi(P(\mathbf{S}, \mathbf{X}, A|G = o), P(\mathbf{S}, \mathbf{X}, A|G = e)), \quad (11)$$

and

$$OT(P(\mathbf{S}, \mathbf{X}, A|G = o), P(\mathbf{S}, \mathbf{X}, A|G = e)) \leq m\text{-}OT(P(\mathbf{S}, \mathbf{X}, A|G = o), P(\mathbf{S}, \mathbf{X}, A|G = e)). \quad (12)$$

Proof. Assuming the probability measure of $P(\mathbf{S}, \mathbf{X}, A|G = o)$ and $P(\mathbf{S}, \mathbf{X}, A|G = e)$ are α, β , respectively. Then according to the definition, the proof of Eq. (11) is equivalent to prove:

$$\left(\frac{1}{k} \sum_{i=1}^k \Gamma_i \right) \mathbf{1}_{n_e} = \alpha, \quad \left(\frac{1}{k} \sum_{i=1}^k \Gamma_i \right)^T \mathbf{1}_{n_o} = \beta.$$

Note that $\gamma_i \in \Pi(P_{\mathcal{B}_i}(\mathbf{S}, \mathbf{X}, A|G = o), P(\mathbf{S}, \mathbf{X}, A|G = e))$ satisfies:

$$\gamma_i \mathbf{1}_{n_e} = \alpha_{\mathcal{B}_i}, \quad \gamma_i^T \mathbf{1}_b = \beta.$$

Combining it with the definition of Γ_i , we have:

$$\Gamma_i \mathbf{1}_{n_e} = \bar{\alpha}_{\mathcal{B}_i} = \eta_i \odot \alpha, \quad (13)$$

$$\Gamma_i^T \mathbf{1}_{n_o} = \beta, \quad (14)$$

where $\bar{\alpha}_{\mathcal{B}_i} \in \mathbb{R}^{n_o}$ is the extension of $\alpha_{\mathcal{B}_i}$ by padding zero entries to the dimension whose index does not belong to \mathcal{B}_i , \odot corresponds to entry-wise product and η_i is a n_o dimensional vector with element satisfying that:

$$\eta_i^j = \begin{cases} \frac{n_o}{b} = k, & \text{if } j \in \mathcal{B}_i, \\ 0, & \text{otherwise.} \end{cases} \quad (15)$$

According Eq. (13) and (14), we have:

$$\left(\frac{1}{k} \sum_{i=1}^k \Gamma_i \right) \mathbf{1}_{n_e} = \frac{1}{k} \sum_{i=1}^k (\Gamma_i \mathbf{1}_{n_e}) = \left(\frac{1}{k} \sum_{i=1}^k \eta_i \right) \odot \alpha, \quad (16)$$

$$\left(\frac{1}{k} \sum_{i=1}^k \Gamma_i \right)^T \mathbf{1}_{n_o} = \frac{1}{k} \sum_{i=1}^k (\Gamma_i^T \mathbf{1}_{n_o}) = \frac{1}{k} \sum_{i=1}^k \beta = \beta,$$

Combining Eq. (15) with conditions $\mathcal{B}_i \cap \mathcal{B}_j = \emptyset$ and $\cup_{i=1}^k \mathcal{B}_i = \{1, 2, \dots, n_o\}$, we obtain that:

$$\left(\frac{1}{k} \sum_{i=1}^k \eta_i \right)^j = k \sum_{i=1}^k \mathbb{I}(j \in \mathcal{B}_i) = k,$$

which means that the term $\frac{1}{k} \sum_{i=1}^k \eta_i$ in Eq. (16) is $\frac{1}{k} \sum_{i=1}^k \eta_i = \mathbf{1}_{n_o}$. As a result, we have already proved Eq. (11) because the following definition holds:

$$\left(\frac{1}{k} \sum_{i=1}^k \Gamma_i \right) \mathbf{1}_{n_e} = \alpha, \quad \left(\frac{1}{k} \sum_{i=1}^k \Gamma_i \right)^T \mathbf{1}_{n_o} = \beta.$$

By denoting the cost matrix between $P(\mathbf{S}, \mathbf{X}, A|G = o)$ and $P(\mathbf{S}, \mathbf{X}, A|G = e)$ as C , the above definition also leads to the following inequality:

$$\begin{aligned} & OT(P(\mathbf{S}, \mathbf{X}, A|G = o), P(\mathbf{S}, \mathbf{X}, A|G = e)) \\ & \leq \left\langle \frac{1}{k} \sum_{i=1}^k \Gamma_i, C \right\rangle = \frac{1}{k} \sum_{i=1}^k \langle \Gamma_i, C \rangle \\ & = \frac{1}{k} \sum_{i=1}^k OT(P_{\mathcal{B}_i}(\mathbf{S}, \mathbf{X}, A|G = o), P(\mathbf{S}, \mathbf{X}, A|G = e)) \\ & = m\text{-}OT(P(\mathbf{S}, \mathbf{X}, A|G = o), P(\mathbf{S}, \mathbf{X}, A|G = e)), \end{aligned} \quad (17)$$

where the Eq. (17) comes from the definition of Γ_i . So far, we have finished the proof of Eq. (12). \square

A.5 Proof of Theorem 4

Theorem 4. Assuming a family \mathcal{M} of function $m : \mathcal{Z} \times \mathcal{A} \rightarrow \mathbb{R}$, and there exists a constant $B_\Phi > 0$ such that $\frac{1}{B_\Phi} \cdot \ell_{\phi,g,h}(\mathbf{x}, a) \in \mathcal{M}$, then we have:

$$\mathcal{E}_{cf} \leq \mathcal{E}_f^{\mathbf{w}_o} + \text{IPM}_{\mathcal{M}}(P(\mathbf{Z})P(A), \mathbf{w}_o \cdot P(\mathbf{Z}, A)),$$

where $\text{IPM}_{\mathcal{M}}(p, q) = \sup_{m \in \mathcal{M}} \left| \int_{\mathcal{X}} g(x)(p(x) - q(x))dx \right|$ is integral probability metric for a chosen \mathcal{M} , $P(\mathbf{Z})$ and $P(\mathbf{Z}, A)$ are distributions induced by the map ϕ from $P(\mathbf{X})$ and $P(\mathbf{X}, A)$.

Proof. The inequality is equivalent to

$$\begin{aligned} \mathcal{E}_{cf} - \mathcal{E}_f^{\mathbf{w}_o} &= \int_{\mathcal{X}} \int_{\mathcal{A}} P(\mathbf{x})P(a)\ell_{\phi,g,h}(\mathbf{x}, a) dxda - \int_{\mathcal{X}} \int_{\mathcal{A}} P^{\mathbf{w}_o}(\mathbf{x}, a)\ell_{\phi,g,h}(\mathbf{x}, a) dxda \\ &= \int_{\mathcal{X}} \int_{\mathcal{A}} (P(\mathbf{x})P(a) - P^{\mathbf{w}_o}(\mathbf{x}, a)) \ell_{\phi,g,h}(\mathbf{x}, a) dxda \\ &= \int_{\mathcal{Z}} \int_{\mathcal{A}} (P(\mathbf{z})P(a) - P^{\mathbf{w}_o}(\mathbf{z}, a)) \ell_{\phi,g,h}(\psi(\mathbf{z}), a) dzda \end{aligned} \quad (18)$$

$$\begin{aligned} &\leq \sup_{m \in \mathcal{M}} \left| \int_{\mathcal{Z}} \int_{\mathcal{A}} (P(\mathbf{z})P(a) - P^{\mathbf{w}_o}(\mathbf{z}, a)) m(\mathbf{z}, a) dzda \right| \\ &= \text{IPM}_{\mathcal{M}}(P(\mathbf{Z})P(A), P^{\mathbf{w}_o}(\mathbf{Z}, A)) \\ &= \text{IPM}_{\mathcal{M}}(P(\mathbf{Z})P(A), \mathbf{w}_o \cdot P(\mathbf{Z}, A)), \end{aligned} \quad (19)$$

where Eq. (18) can be obtained by the standard change of variables formula, using the determinant of the Jacobian of $\psi(\mathbf{z})$, Eq. (19) is according to the definition of IPM with the assumption that $\frac{1}{B_\Phi} \cdot \ell_{\phi,g,h}(\mathbf{x}, a) \in \mathcal{M}$. \square

B Derivation about Projected Mirror Descent

In this section, following [58], we develop a projected mirror descent [40, 43] based on the Kullback-Leibler (KL) divergence to solve the following problem, which is non-trivial to address because of the equality constraints:

$$\begin{aligned} &\min_{\mathbf{w}_{o,B}} \min_{\gamma \in \Pi(\alpha_B, \beta)} \langle \gamma, \mathbf{C} \rangle + \lambda_e \Omega(\gamma), \\ &s.t. \Pi(\alpha_B, \beta) = \{\gamma \in \mathbb{R}^{b \times n_e} | \gamma \mathbf{1}_{n_e} = \mathbf{w}_{o,B}, \gamma^T \mathbf{1}_b = \boldsymbol{\mu}, \gamma_{ij} \in [0, 1]\}, \end{aligned}$$

Firstly, we rewrite the constrain about γ as

$$\Pi'(\alpha_B, \beta) = \{\gamma \in \mathbb{R}^{b \times n_e} | \gamma^T \mathbf{1}_b = \boldsymbol{\mu}, \gamma_{ij} \in [0, 1]\}, \quad (20)$$

which does not consider the constraint $\gamma \mathbf{1}_{n_e} = \mathbf{w}_{o,B}$ since $\mathbf{w}_{o,B}$ are also parameters to be optimized. Based on this, the OT problem with a negative entropy regularization is given as follows:

$$\min_{\gamma} \langle \gamma, \mathbf{C} \rangle + \lambda_e \Omega(\gamma), \quad s.t. \gamma \in \Pi'(\alpha_B, \beta). \quad (21)$$

For simplicity, we define the objective function in Problem (21) as

$$f(\gamma) = \langle \gamma, \mathbf{C} \rangle + \lambda_e \Omega(\gamma),$$

and the (i, j) -th element of the gradient $\nabla f(\gamma)$ is denoted by ∇_{ij} ,

$$\nabla_{ij} = C_{ij} + \lambda_e \log w_i = C_{ij} + \lambda_e \log \gamma_i,$$

where γ_i is the sum of i -th row of γ . Then at each iteration, we solve the following problem:

$$\gamma^k = \min_{\gamma \in \Pi'(\alpha_B, \beta)} \eta \langle \nabla f(\gamma^{k-1}), \gamma \rangle + \mathcal{D}(\gamma || \gamma^{k-1}), \quad (22)$$

which firstly performs proximal gradient descent with the Bregman divergence and the stepsize η , and then obtains a feasible solution in the set $\Pi'(\alpha_B, \beta)$ by projection. Next, we present the details of these two operations.

Proximal Gradient Descent Let v^k be the solution to Problem (22) without considering the constraint $\gamma \in \Pi'(\alpha_B, \beta)$, i.e.,

$$v^k = \min_{\gamma} \eta \langle \nabla f(\gamma^{k-1}), \gamma \rangle + \mathcal{D}(\gamma \| \gamma^{k-1}).$$

We adopt the KL divergence between two distributions γ and γ^{k-1} as the Bregman divergence $\mathcal{D}(\gamma \| \gamma^k)$, then the closed-form solution to the above problem is given as:

$$v^k = \gamma^{k-1} \odot \exp(-\eta \nabla f(\gamma^{k-1})). \quad (23)$$

Projection Operation To make sure γ^k satisfies the constraints in Eq. (20), we update γ^k by finding $\gamma \in \Pi'(\alpha_B, \beta)$ which is most close to v^k under the KL metric. This is achieved by solving the following projection problem (ignore constraint $\gamma_{ij} \in [0, 1]$ for now):

$$\min_{\gamma} \mathcal{D}(\gamma \| v^k) = \sum_{i=1}^b \sum_{j=1}^{n_e} \gamma_{ij} \log\left(\frac{\gamma_{ij}}{v_{ij}^k}\right) - \gamma_{ij} + v_{ij}^k, \quad s.t. \quad \gamma^\top \mathbf{1}_b = \boldsymbol{\mu}. \quad (24)$$

By introducing the Lagrangian multipliers $\boldsymbol{\lambda} = [\lambda_1, \dots, \lambda_{n_e}]^\top$ for the equality constraint $\gamma^\top \mathbf{1}_b = \boldsymbol{\mu}$, we obtain the Lagrangian $\mathcal{L}(\gamma, \boldsymbol{\lambda})$ as follows:

$$\mathcal{L}(\gamma, \boldsymbol{\lambda}) = \sum_{i=1}^b \sum_{j=1}^{n_e} \gamma_{ij} \log\left(\frac{\gamma_{ij}}{v_{ij}^k}\right) - \gamma_{ij} + v_{ij}^k + \boldsymbol{\lambda}^\top (\gamma^\top \mathbf{1}_b - \boldsymbol{\mu}).$$

By taking the partial derivative of $\mathcal{L}(\gamma, \boldsymbol{\lambda})$ with respect to γ_{ij} to zero, we obtain:

$$\begin{aligned} \log \gamma_{ij} &= \log v_{ij}^k - \lambda_j \\ \Rightarrow \gamma_{ij} &= v_{ij}^k \exp(-\lambda_j). \end{aligned} \quad (25)$$

According to the equality constraint $\gamma^\top \mathbf{1}_b = \boldsymbol{\mu}$, we have $\sum_{i=1}^b \gamma_{ij} = 1/n_e$. Combining it with the above result, we further obtain:

$$\begin{aligned} \sum_{i=1}^b \gamma_{ij} &= \sum_{i=1}^b v_{ij}^k \exp(-\lambda_j) = \exp(-\lambda_j) \sum_{i=1}^b v_{ij}^k = \frac{1}{n_e} \\ \Rightarrow \exp(-\lambda_j) &= \frac{1}{n_e \sum_{i=1}^b v_{ij}^k}. \end{aligned} \quad (26)$$

Combining Eq. (25) and (26), we obtain the closed-form solution:

$$\gamma_{ij} = v_{ij}^k / \left(n_e \sum_{i=1}^b v_{ij}^k \right). \quad (27)$$

For an initial value $\gamma_{ij}^0 \geq 0$, given $v_{ij}^k > 0$ which is guaranteed by the update rule in Eq. (20), it is obvious that the solution obtained by Eq. (27) satisfies the box constraint $\gamma_{ij} \in [0, 1]$. Therefore, Problem (24) does not consider this constraint explicitly.

For now, we have derived how to solve the Problem Eq. (21). That is, we repeat steps Eq. (23) and (27) until converging.

C Additional Related Work

Since our work is also close to work that considers continuous treatment. We provide additional related work to them as follows.

Dose-Response Curve Estimation Dose-response curve estimation is broadly studied through statistical methods [51, 35, 61], and most of them are based on the generalized propensity score (GPS)

Algorithm 1 Pseudocode of the proposed LEARN

Require: Observational dataset O , experimental dataset E , initial model parameters $\theta = \{\theta_\phi, \theta_q(a), \theta_g(a), \theta_f(a), \theta_h(a)\}$, hyper-parameters $\{\lambda_o, \lambda_b, \lambda_e\}$, batch size b , pre-training epoch n_{pre} , training epoch n , OT epoch n_{ot} , learning rate α

- 1: // *Pre-training phase. Ensuring the short-term embeddings of RNN are meaningful, which will be used in constructing the cost matrix C in optimal transport at each training iteration*
- 2: **for** $i = 1, 2, \dots, n_{pre}$ **do**
- 3: Sample a mini-batch \mathcal{B} from the observational dataset O
- 4: Update $\theta^{i+1} \leftarrow \theta^i - \alpha \nabla_{\theta} \mathcal{L}_{\theta}$ by setting $\mathbf{w}_{\mathcal{B}} = \{\frac{1}{b}, \frac{1}{b}, \dots, \frac{1}{b}\}$.
- 5: **end for**
- 6: // *Training phase. Removing the observed and unobserved confounding bias*
- 7: **for** $i = 1, 2, \dots, n$ **do**
- 8: Sample a mini-batch \mathcal{B} from the observational dataset O
- 9: // *Learning weights $\mathbf{w}_{\mathcal{B}}$ for the batch observational units via data combination*
- 10: Compute the cost matrix C between \mathcal{B} and E
- 11: **for** $k = 1, 2, \dots, n_{ot}$ **do**
- 12: Calculate v^k according to Eq. (23)
- 13: Update γ^k according to Eq. (27)
- 14: **end for**
- 15: $\hat{\mathbf{w}}_{\mathcal{B}} = \gamma^k \mathbf{1}_{n_e}$
- 16: // *Weighted regression with IPM term*
- 17: Update $\theta^{i+1} \leftarrow \theta^i - \alpha \nabla_{\theta} \mathcal{L}_{\theta}$ by setting $\mathbf{w}_{\mathcal{B}} = \hat{\mathbf{w}}_{\mathcal{B}}$.
- 18: **end for**
- 19: **return** Learned model parameters θ

[31] or the entropy balancing for continuous treatments (EBCT) [49]. Recently, deep learning-based methods also attract the attention of the research community. DRNet [45] divides the continuous treatment into several intervals, and trains one separate head for each interval. In order to produce a continuous curve, VCNet [41] adapts a varying coefficient model into neural networks to handle the continuous treatment. SCIGAN [7] generates counterfactual outcomes for continuous treatments based on the generative adversarial network (GAN) framework. ADMIT [56] derives a counterfactual bound of estimating the average dose-response curve with a discretized approximation of the IPM distance, and ACFR [34] minimizes the KL-divergence using an adversarial game to extract balanced representations for continuous treatment. Different from existing works, we aim to estimate the HDRC under the long-term estimation scenario in this paper.

D Model Details

Implementation Details Our code is implemented using the PyTorch 1.8.1 framework. Note that all MLP in our model is 2 fully connected layers with 50 hidden units and Elu activation function, then we build our model as follows:

For the *balanced representation module*, we use an MLP to build the representation function ϕ , and use the Wasserstein distance as the IPM term. The code of the Wasserstein distance can be found in <https://github.com/rguo12/network-deconfounder-wsdm20/blob/master/utills.py>.

For the *OT weight module*, at each iteration, we first construct the cost matrix as $C_{ij} = \beta_r d(\bar{\mathbf{r}}_i, \bar{\mathbf{r}}_j) + \beta_x d(\mathbf{x}_i, \mathbf{x}_j) + \beta_a d(a_i, a_j)$, where the hyperparameters $\beta_r = 10, \beta_x = 0.1, \beta_a = 0.1$, $d(\cdot, \cdot)$ is the euclidean distance, and the distance of short-term outcomes is calculated from the mean embedding of RNN as $\bar{\mathbf{r}} = \frac{1}{t_0} \sum_{t=1}^{t_0} \mathbf{r}_t$. After that, we obtain the optimal transport probability matrix γ^* by repeating steps Eq. (23) and (27) in Appendix B until converging. Finally, the weights of observational samples could be obtained as $w_i = \sum_{j=1}^{n_e} \gamma_{ij}^*$, where w_i is the sum of the i -th row of γ^* .

For the *long-term estimation module*, we use a shared MLP to build the function $g(\cdot)$ predicting the short-term outcomes, use another MLP to build the function $h(\cdot)$ predicting the long-term outcome, and use a bidirectional GRU model to build the RNN $q(\cdot)$ extracting the short-term representations.

As for the attention mechanism $f(\cdot)$, we implement it as follows:

$$\tilde{\mathbf{R}}_t = \tanh(\mathbf{W}\mathbf{R}_t + \mathbf{b}), \quad \alpha_t = \frac{\exp \tilde{\mathbf{R}}_t^\top \mathbf{V}}{\sum_{t=1}^{t_0} \exp \tilde{\mathbf{R}}_t^\top \mathbf{V}}, \quad \mathbf{R}_T = \sum_{t=1}^{t_0} \alpha_t \mathbf{R}_t,$$

where $\mathbf{W}, \mathbf{b}, \mathbf{V}$ are the parameters of the attention mechanism $f(\cdot)$.

Further, following [41], we model the parameters $\theta(a)$ of the above four network structures $q(\cdot), g(\cdot), f(\cdot), h(\cdot)$ as the varying coefficient structure, i.e., $\theta(a) = \sum_{l=1}^L \alpha_l \phi_l(a)$, where ϕ_l is the basis function and α_l is the coefficient. Specifically, we use truncated polynomial basis with degree 2 and two knots at $\{1/3, 2/3\}$ (altogether 5 basis) to build the varying coefficient structure. The code of the varying coefficient structure is written based on VCNet (https://github.com/lushleaf/varying-coefficient-net-with-functional-tr/blob/main/models/dynamic_net.py).

Parameters Setting We set the hyperparameters in our model as follows: the strength of the Wasserstein distance $\lambda_b \in \{50, 100, 150, 200\}$, the strength of negative entropy regularization $\lambda_b = 100$, the learning rate about the projected mirror descent as 0.001, and the iterations about the projected mirror descent as $\{50, 100, 500\}$, the strength of short-term outcome loss as $\lambda_o \in \{0.25, 0.5, 0.75\}$. Besides, we pre-train the model for 100 epochs without weighting, and then the number of training epochs is 400 with an early stop. We use Adam optimizer [36] with a learning rate of $1e-3$ and weight decay of $5e-4$. All the experiments are run on the Tesla P40 GPU.

Pseudocode We provide the pseudocode of our model in Algorithm 1.

E Experimental Details

E.1 Dataset Generation

Synthetic Data Generation We simulate synthetic data as follows. For each observational unit $i \in \{1, 2, \dots, n_o\}$ with $G = o$, we generate p observed covariates and q unobserved covariates from independent identical distributions, i.e., $X^o \sim \mathcal{N}(\mathbf{0.1}_p, \mathbf{I}_p)$ and $U \sim \mathcal{N}(\mathbf{0.25}_q, \mathbf{I}_q)$, where \mathbf{I} denotes the identity matrix. Similarly, we generate experimental units $i \in \{1, 2, \dots, n_e\}$ with $G = e$ as $X^e \sim \mathcal{N}(\mathbf{0.5}_p, \mathbf{I}_p), U \sim \mathcal{N}(\mathbf{0.25}_q, \mathbf{I}_q)$. Then we generate treatment and outcomes for two types of datasets using the following rules with $W_j^t \sim \mathcal{U}(0, 0.5), W_j^y \sim \mathcal{U}(0.5, 1)$:

$$A = \sigma\left(\sum_{j=1}^{p/3} W_j^t \sin X_j + \sum_{j=p/3}^{2p/3} W_j^t X_j^2 + \beta_U \bar{U} \mathbb{I}(G = o)\right),$$

$$Y_t = \sum_{j=p/3}^{2p/3} W_j^y X_j^2 + (t+5)A\left(\sum_{j=2p/3}^p W_j^y X_j\right) + \frac{\beta_U t A}{5} \left(\sum_{j=1}^q W_j^y \cos U_j\right) + 0.25 \bar{Y}_{1:t-1} + \mathcal{N}(0, 0.5),$$

where $n_o = 10000, n_e = 500, p = 15, q = 5$. We denote short-term outcomes as $\mathbf{S} = \{Y_1, Y_2, \dots, Y_7\}$ and long-term outcome as $Y_T = Y_{14}$. Besides, we design 5 simulation datasets with varying $\beta_U \in \{1, 1.25, 1.5, 1.75, 2\}$ that controls different strengths of unobserved confounding bias.

Semi-synthetic Data Generation In semi-synthetic datasets News and TCGA, we reuse their covariates. Firstly, we randomly partition the dataset into observational ($G = o$) and experimental ($G = e$) subsets at a 9:1 ratio, followed by segregation of original covariates into observed (X) and unobserved (U) ones at an 8:2 ratio. Then we follow [41, 56] to generate the assigned treatments and their corresponding outcomes. After generating a set of parameters $\mathbf{v}_{i,x/u} = \mathbf{u}_{i,x/u} / \|\mathbf{u}_{i,x/u}\|$ and $i = 1, 2, 3$, where $\mathbf{u}_{i,x/u}$ is sampled from a normal distribution $\mathcal{N}(\mathbf{0}, \mathbf{1})$, we have:

$$A \sim \text{Beta}(\gamma, \beta), \text{ where } \gamma = 2, \beta = \frac{\gamma - 1}{d^*} + 2 - \gamma \text{ and } d^* = \left| \frac{\mathbf{v}_{3,x}^T X}{2\mathbf{v}_{2,x}^T X} + \frac{\mathbf{v}_{3,u}^T U}{2\mathbf{v}_{2,u}^T U} \mathbb{I}(G = o) \right|,$$

$$Y_t \sim \mathcal{N}(\mu, 0.5), \text{ where } \mu = 4(A - 0.5)^2 \times \sin\left(\frac{\pi}{2}A\right) \times 2(\max(-2, \exp\left(\frac{\mathbf{v}_{2,x}^T X}{\mathbf{v}_{3,x}^T X} + \frac{\mathbf{v}_{2,u}^T U}{\mathbf{v}_{3,u}^T U} - 0.3\right))$$

$$+ 20A(\mathbf{v}_{1,x}^T X + \mathbf{v}_{1,u}^T U)) + 0.5 \bar{Y}_{1:t-1}.$$

Same as the synthetic data generation, we collect $\mathbf{S} = \{Y_1, Y_2, \dots, Y_7\}$ and $Y_T = Y_{14}$.

E.2 Hyperparameter Sensitivity Study

We investigate the role of three hyperparameters in our model: λ_o , λ_b , λ_e , and the results are shown in Fig. 3. Firstly, we observe that MISE increases when λ_b becomes small or large, indicating that there exists a trade-off between eliminating observed confounding bias and estimating outcomes accurately. Secondly, the results of varying λ_o shows that considering the short-term outcomes of observational and experimental datasets together can bring a certain degree of improvement. Finally, applying the negative entropy regularization in OT can bring a slight improvement, and the performance of our model with different strengths is relatively stable.

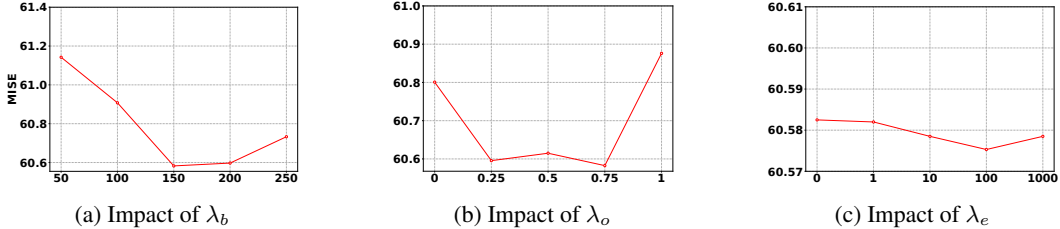


Figure 3: Hyperparameter sensitivity. (a) Strength of IPM. (b) Strength of short-term loss between observational and experimental datasets. (c) Strength of negative entropy regularization.

F Broader Impact and Limitations

This paper studies the problem of estimating the long-term HDRC, which utilizes the power of deep learning and optimal transport technologies to assist better long-term decision-making in many domains. For example, in a ride-hailing platform, the platform needs to evaluate the effect of various incomes of different drivers on their retention after one year to keep the long-term balance of demand and supply. In the medical field, a healthcare institution might need to analyze the impact of a new medication on the five-year survival rates of cancer patients to determine whether to adopt it as a standard treatment protocol. However, this technology towards better estimating and understanding long-term HDRC can be used negatively, where someone wishing to cause harm can use the estimated outcomes to select the worst outcome.

At the same time, although this work allows there exist unobserved confounders in the observational dataset, some standard assumptions in causal inference are still needed. For example, this work assumes the Positivity Assumption holds, and this assumption may be violated in some real-world scenarios when there exist units that only receive treatment $A = a$, e.g., in some cases, critically ill patients have to be treated, leading to no samples of untreated critically ill patients. Also, this work still relies on the existence of an experimental dataset to remove unobserved confounding, and how to estimate long-term HDRC only with a confounded observational dataset can be further explored.